

## GEOCHEMICAL PROPERTIES OF SEEPAGE-FILTRATION AND FRACTURE SPRINGS IN WISCONSIN

SUSAN SWANSON, Beloit College  
OCEAN CLEVETTE, Beloit College, Peer Mentor

### INTRODUCTION

A wide variety of geologic and topographic settings, flow mechanisms, discharge rates, and physicochemical conditions have been documented for springs (Stevens et al., 2021). For any given spring, conditions within the spring environment may also be spatially variable, contributing to the diversity of spring biota. For example, macroinvertebrates can be very diverse in springs with microhabitats and heterogeneous substrates (Glazier, 2009). Yet, studies of spring water temperature and geochemistry often rely on sensors installed at the spring orifice or samples collected at a single position, and values are assumed to be representative of the entire spring environment (e.g., Luhman et al., 2011; Swanson et al., 2020). The spatial variability of temperature in the immediate spring environment has recently been shown to vary by spring source geomorphology. At fracture springs, groundwater flows from discrete sources and the distribution of temperature is spatially consistent, whereas at seepage-filtration springs, groundwater flows in a more diffuse manner from numerous openings in permeable material and the distribution of temperature is more spatially variable (Fig. 1) (Swanson and Graham, 2022).

In the summer of 2021, we undertook a four-student Keck Gateway project to evaluate relationships between the spatial variation of geochemical conditions and spring source geomorphology. Students selected six springs from over 400 springs inventoried in Wisconsin (Swanson et al., 2019). Some springs in Wisconsin exhibit more than one type of source geomorphology. Those selected for this study are exclusively fracture or exclusively seepage-filtration springs, the two most common spring source

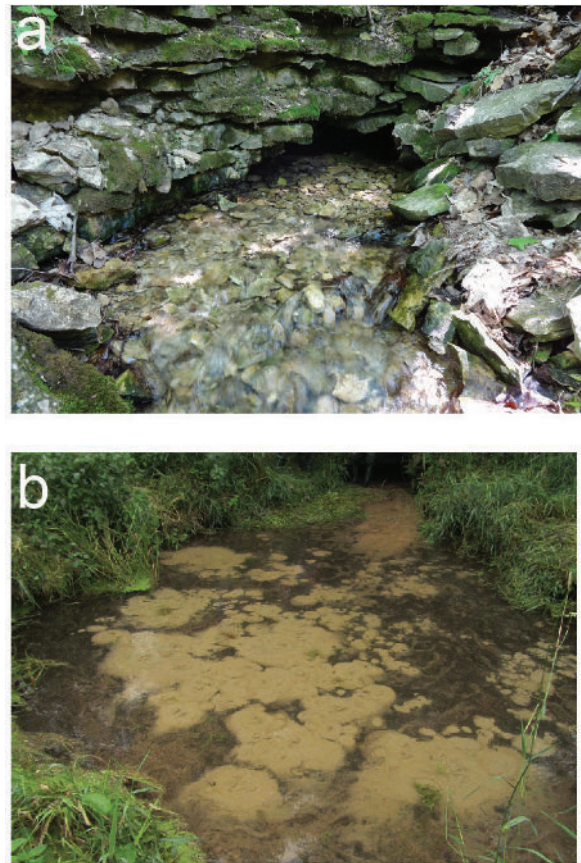


Figure 1. A typical fracture spring (a.), where groundwater flows from a discrete fracture and a typical seepage-filtration spring (b.), where groundwater flows from numerous openings in permeable, unlithified material.

geomorphologies in the region and those which have distinct differences in spatial distribution of temperature (Fig. 2).

Most fracture springs in Wisconsin are found in the Driftless Area of southwestern Wisconsin. They form as a result of preferential groundwater flow through bedding-plane fractures in exposed or shallowly buried and mostly horizontal Paleozoic sedimentary strata composed of sandstone, shale, limestone, and dolomite. Seepage-filtration springs in Wisconsin

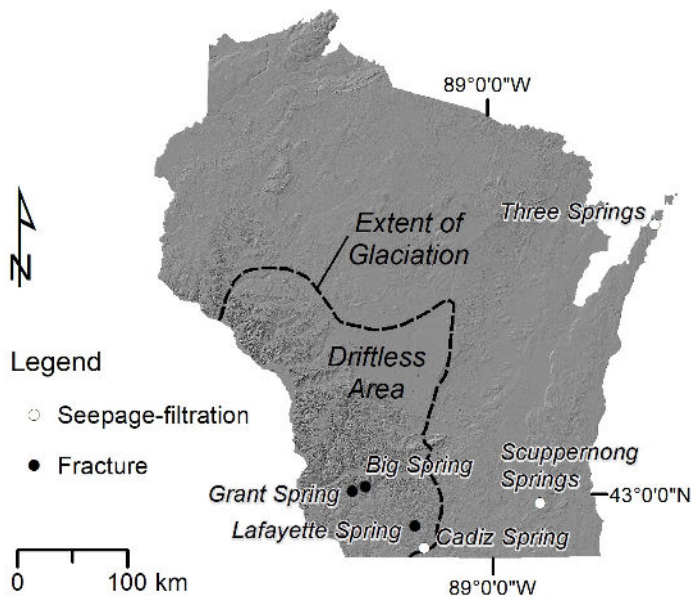


Figure 2. The three fracture springs and three seep-filtration springs utilized in this study.

are a result of variations in topography and lithology of surficial unlithified materials. They commonly form where groundwater emerges at the base of glacial moraines or near the margins of former glacial lakebeds (Swanson et al. 2019).

## METHODS

Students worked as a team to document site environmental conditions, measure geochemical concentrations across the spring pool, collect water samples for laboratory analysis, image the water surface for temperature conditions, and measure spring flow (Fig. 3). They carefully drafted to-scale site maps by making measurements of the dimensions of the spring pool and noting physical features, such as the spring orifice, exposed bedrock, boulders, or vegetation. Photo points are noted on the maps, as well as GPS and discharge measurement positions and water quality sampling locations.

Once the students were familiar with the immediate spring environment, they could assess and design an optimal sampling array for the site. Sampling arrays were positioned as close to each spring orifice as possible. All sites used a sample grid spacing of 30 cm; however, the total length and width of each sampling array depended on the dimensions of the spring pool. At each sampling grid point, students measured water depth using a meter stick and



Figure 3. Students worked as a team to (a.) measure geochemical properties along a transect within a sampling array, (b.) measure spring discharge using a wading rod and flow meter, and (c.) sample groundwater after field-filtering.

measured water pH, specific conductance ( $\mu\text{mhos/cm}$ ,  $25^\circ\text{C}$ ), and temperature ( $^\circ\text{C}$ ) using a YSI 600 XLM Multiparameter Water Quality Sonde. They also collected water samples at each grid point using a small hand pump. The samples were kept on ice during transport and then analyzed within 24 hours for Chloride (Cl) and Nitrate ( $\text{NO}_3\text{-N}$ ) concentrations using Vernier ion-specific electrodes. Because spring water samples are most commonly collected at a single position as close to emerging groundwater as possible, students also collected a water sample in a position such as this at each spring. This approach allowed for comparisons between the single sample and the sampling array concentrations. Water for the single sample was filtered using a handheld vacuum pump with a  $0.45\ \mu\text{m}$  filter and shipped on ice to the University of Wisconsin-Stevens Point Water and Environmental Analysis Lab for analysis of major ions and alkalinity.

After water quality sampling was completed, students used a FLIR Vue Pro 640 camera to capture thermal images in the vicinity of the sampling array and spring orifice. This process allowed students to

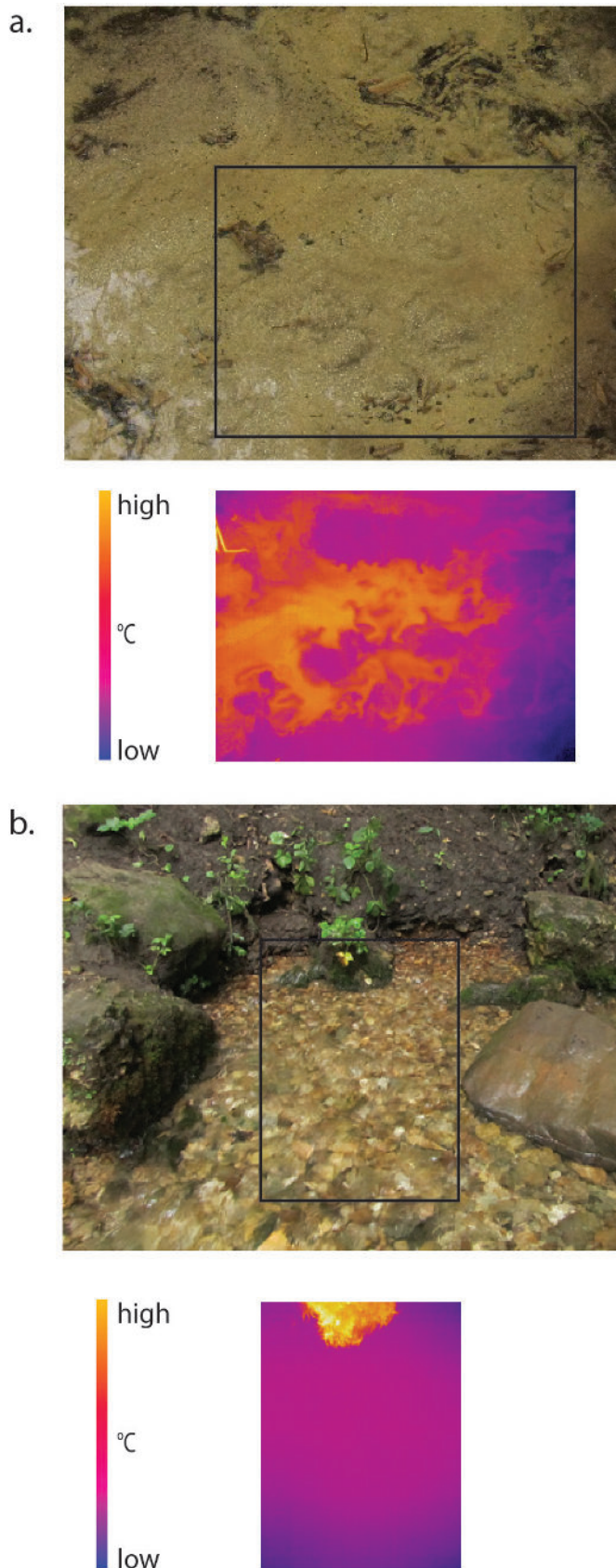


Figure 4. Examples of digital and thermal images for (a.) a seepage-filtration spring (Three Springs) and (b.) a fracture spring (Big Spring). The black rectangles show the approximate positions of the thermal images. Each thermal image is approximately 0.6 m by 1 m.

confirm the results of Swanson et al. (2022) for their own field sites. Fieldwork was conducted in July, so differences between spring pool surface water and emerging groundwater temperatures are likely to be at a maximum. A range pole, tripod, and overhead camera boom positioned the thermal camera 90° from and 1.2 m above the water surface. The camera has a 45° field of view (FOV), which results in a lateral distance across the bottom of the thermal images of about 1 m. Images are composed of 640 x 512 pixels, so the effective pixel size of each image is 2.4 mm<sup>2</sup>. Students shaded the spring pool with a large tarp to minimize reflected radiation from clouds and tree canopy.

Finally, spring discharge was measured and calculated using a flow meter and the velocity area method or measured directly using a cutthroat flume. The measurement approach depended on the width of the spring channel and the depth of water.

As in the field, students worked as a team to catalog and analyze their field and laboratory results. They tabulated measurements and uploaded them to ArcGIS where the spatial distribution of geochemical characteristics (pH, specific conductance, Chloride, Nitrate-N) could be mapped for each site using the Inverse Distance Weighted method.

## FINDINGS

All six springs under study are rheocrenes, or stream-forming springs. Three are fracture springs and three are seepage-filtration springs. The immediate spring environments, or spring pool areas, for all of the springs are relatively small (less than 70 m<sup>2</sup>) and water depths are shallow (less than 50 cm). Discharge for the springs ranged from  $6.3 \times 10^{-3}$  to  $4.6 \times 10^{-1}$  m<sup>3</sup>/sec with an average of  $1.5 \times 10^{-1}$  m<sup>3</sup>/sec. All six springs have experienced disturbance from agriculture, recreation, or roads.

Thermal images support the previous work by Swanson and Graham (2022) by showing that the spatial distribution of temperature differs between spring types, with greater variation at seepage-filtration springs (Fig. 4). Temperature varied by up to 6.5°C across the surface of the seepage-filtration springs, whereas it varied by no more than 2°C across

the surface of the fracture springs.

Specific conductance (25°C) was very consistent at the fracture springs, varying by only 2 to 3  $\mu\text{mhos/cm}$  across the sampling arrays. Specific conductance at the seepage-filtration springs varied by 14 to 20  $\mu\text{mhos/cm}$  across the sampling arrays (Fig. 5a., Table 1). Students noted less distinct differences between fracture springs and seepage-filtration for pH and Chloride concentrations, but patterns may still exist. The pH at the fracture springs varied by 0 to 0.1 pH across the sampling arrays, whereas it varied by 0.1 to 0.7 pH units across the sampling arrays at the seepage-filtration springs (Fig. 5b., Table 1). Similarly, Chloride concentrations were somewhat more consistent at the fracture springs. The ranges in concentrations were 0.2 to 2.9 mg/L at the fracture springs and 0.4 to 8.5 mg/L at the seepage-filtration springs (Fig. 5c., Table 1). Ranges in Nitrate-N concentrations were similar across all six sites (Fig. 5d., Table 1). However, due to instability during measurements, students suspected that the Nitrate-N electrode may have been less accurate.

In light of the field results for Chloride and Nitrate-N, the results of the lab-analyzed single position samples for each site were compared to average field Chloride and Nitrate-N concentrations. In both cases, field values were somewhat higher than lab values, but there was a stronger linear relationship between lab and field values for Chloride samples ( $R^2 = 0.8$ ) versus Nitrate-N samples ( $R^2 = 0.6$ ), further suggesting that the Nitrate-N ion-specific electrode may have been less reliable.

On the basis of their results, the students concluded that their results were promising and that they supported the idea that a single sampling point is unlikely to capture the range of geochemical and habitat characteristics in springs, especially for seepage-filtration springs. However, they also agreed on the need for further investigation. Additional fracture and seepage-filtration springs should be investigated, resulting in an ability to calculate more robust summary statistics. If spring pool area and time permit, the extent of the sampling arrays should be increased and the grid-spacing should be decreased. Repeating the same measurements in different seasons may also capture important temporal, as well as

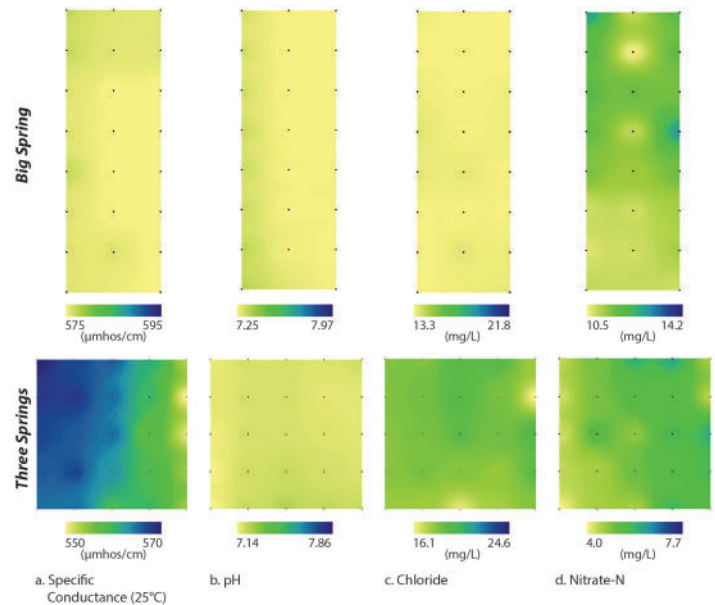


Figure 5. Examples of geochemical maps for a fracture spring (Big Spring) and a seepage-filtration spring (Three Springs). Sampling points, represented by small black dots, are spaced every 30 cm. Minimum and maximum values for each parameter differ between Big Spring and Three Springs, but ranges in values are the same, making comparisons of spatial variation possible.

Table 1. Geochemical results for three seepage-filtration and three fracture springs.

Spring	Specific Conductance ( $\mu\text{mhos/cm}$ , 25°C)		pH		Chloride (mg/L)		Nitrate-N (mg/L)		
	Mean	Range	Mean	Range	Mean	Range	Mean	Range	
Seepage-filtration	Cadiz	553	16	7.3	0.3	24.6	8.5	7.8	0.8
	Scuppermong	576	14	7.5	0.7	32.4	3.0	7.1	0.6
	Three Springs	562	20	7.2	0.1	18.2	0.4	5.1	0.6
Fracture	Grant	534	2	7.2	0.1	9.7	2.9	8.3	0.7
	Big Spring	576	2	7.3	0.1	13.5	0.4	11.4	0.6
	Lafayette	472	3	7.2	0	15.0	1.2	8.4	0.6

spatial, variations in geochemical characteristics.

## ACKNOWLEDGEMENTS

This material is based upon work supported by the Keck Geology Consortium and the National Science Foundation under Grant No. 2050697. Additional funding for this project was generously provided by the Beloit College Geology Department. We thank the private landowners and public land managers who allowed access to the springs.

## REFERENCES

- Glazier, D.S., 2009, Springs. In Likens GE (ed.) Encyclopedia of Inland Waters., Volume 1: Elsevier, Oxford, UK. p. 734–755.
- Luhmann, A.J., Covington, M.D., Peters, A.J., Alexander, S.C., Anger, C.T., Green, J.A., Runkel, A.C., Alexander, E.C. Jr., 2011, Classification of thermal patterns at karst springs and cave streams: Groundwater v. 49, no. 3, p. 324–335. <https://doi.org/10.1111/j.1745-6584.2010.00737.x>
- Stevens, L.E., Schenk, E.R., Springer, A.E., 2021, Springs ecosystem classification: Ecol Appl v. 31, no. 1, p. 1–28. <https://doi.org/10.1002/eap.2218>
- Swanson, S.K., Graham, G.E., 2022. Spring flux as an indicator of source geomorphology, substrata, and temperature conditions in springs, Hydrogeology Journal 30(1), 221-229, <https://doi.org/10.1007/s10040-021-02412-1>.
- Swanson, S.K., Graham, G.E., and Hart, D.J., 2019, An inventory of springs in Wisconsin: Wisconsin Geological and Natural History Survey Bulletin 113, 24p.
- Swanson, S.K., Graham, G.E., and Hart, D.J., 2020, Using reference springs to describe expected flow, temperature, and chemistry conditions for geologically related groups of springs: Environmental & Engineering Geoscience v. 26, no. 3, p. 331-344, <https://doi.org/10.2113/EEG-2312R>.